Examination of the Potential of the Seismic Dilatometer (SDMT) to Estimate *In Situ* Stiffness Decay Curves in Various Soil Types

S. Amoroso, P. Monaco, B.M. Lehane, D. Marchetti

Abstract. This paper illustrates the use of the seismic dilatometer (SDMT) to assess the decay of in-situ stiffness with strain level in different soil types. The approach adopted in this study relies on the ability of the SDMT to provide routinely at each test depth both a *small strain* stiffness (G_0 from V_S) and a *working strain* stiffness (constrained modulus M_{DMT} derived from the usual DMT interpretation). At various test sites, *working strain* DMT moduli are compared with reference stiffness decay curves back-figured from (i) the behavior observed under a full-scale test embankment (at Treporti) or footings (in Texas), (ii) from laboratory tests (at L'Aquila, Fucino plain and Po plain) and (iii) various combinations of in-situ and laboratory testing techniques (Western Australia). Typical ranges of the shear strains γ_{DMT} associated with *working strain* DMT moduli are inferred to assist construction of stiffness - strain decay curves for different soil types.
Keywords: seismic dilatometer, *in situ* stiffness decay curves, working strain stiffness, small strain stiffness.

1. Introduction

Methods for deriving stiffness decay curves (G-γ curves or similar, G = shear modulus, γ = shear strain) from *in situ* tests have been proposed by various Authors e.g. Robertson & Ferrera (1993) and Fahey (1998) used the unload-reload (u-r) cycles from self-boring pressuremeter tests; Mayne *et al.* (1999) and Marchetti *et al.* (2008) employed the SDMT; Elhakim & Mayne (2003) and Mayne (2003) adopted the seismic cone tests (SCPTs) while Lehane & Fahey (2004) combined the SCPT and DMT.

The seismic dilatometer (SDMT) is the combination of the flat dilatometer (DMT) with an add-on seismic module for the measurement of the shear wave velocity V_S. The approach adopted in this study relies on the ability of the SDMT to provide routinely, at each test depth, both the stiffness at *small strains* (the small strain shear modulus G_0 obtained from the shear wave velocity V_S as $G_0 = \rho V_S^2$) and the stiffness at *operative strains* (as represented by the constrained modulus M_{DMT} obtained by the usual DMT interpretation). The potential for these two stiffness values to provide guidance when selecting the G-γ curve of a soil element is examined.

2. Flat Dilatometer Test (DMT)

The flat dilatometer, introduced by Marchetti (1980), consists of a steel blade having a thin, expandable, circular steel membrane mounted on one face. When at rest, the membrane is flush with the surrounding flat surface of the blade. The blade is connected, by an electro-pneumatic tube running through the insertion rods, to a control unit on the surface (Figs. 1a and 1b). The control unit is equipped with pressure gauges, an audio-visual signal, a valve for regulating gas pressure (provided by a tank) and vent valves. The blade is advanced into the ground using common field equipment, i.e. penetrometers normally used for the cone penetration test (CPT) or drill rigs.

The test starts by inserting the dilatometer into the ground. When the blade has advanced to the desired test depth, the penetration is stopped. The operator inflates the membrane and takes, in about 30 sec, two readings: the *A* pressure, required to just begin to move the membrane ("lift-off" pressure), and the *B* pressure, required to expand the membrane center of 1.1 mm against the soil. A third reading *C* ("closing pressure") can also optionally be taken by slowly deflating the membrane soon after *B* is reached. The blade is then advanced to the next test depth, with a depth increment of typically 20 cm.

The interpretation proceeds as follows. First the field readings are used to derive the DMT intermediate parameters material index I_D, horizontal stress index K_D, dilatometer modulus E_D. Then I_D, K_D, E_D are used, by means of commonly used correlations, to estimate the constrained modulus M, the undrained shear strength s_u, the *in situ* earth pressure coefficient K_0 (clays), the overconsolidation ratio *OCR* (clays), the friction angle φ' (sands), the bulk unit weight γ. Consolidation and permeability coefficients may be estimated by performing dissipation tests. The

Sara Amoroso, Researcher, Department of Seismology and Tectonophysics, Istituto Nazionale di Geofisica e Vulcanologia, Italy. e-mail: sara.amoroso@ingv.it.
Paola Monaco, Assistant Professor, Department of Civil, Architectural and Environmental Engineering, University of L'Aquila, Italy. e-mail: paola.monaco@univaq.it.
Barry M. Lehane, Winthrop Professor, School of Civil, Environmental and Mining Engineering, University of Western Australia, Western Australia. e-mail: barry.lehane@uwa.edu.au.
Diego Marchetti, Engineer, Studio Prof. Marchetti, Italy. e-mail: diego@marchetti-dmt.it.
Submitted on March 2, 2014; Final Acceptance on December 15, 2014; Discussion open until April 30, 2015.

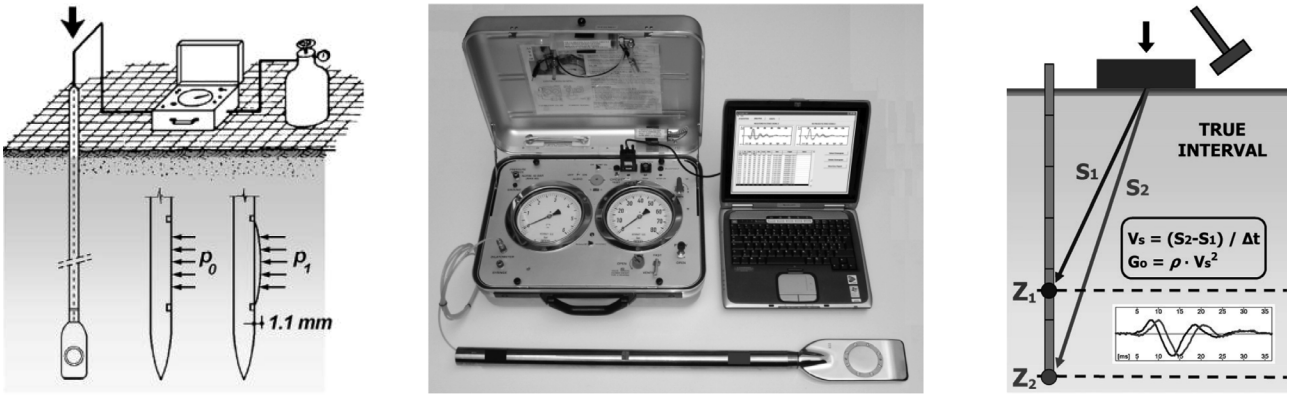

(a) (b) (c)

Figure 1 - (a) Schematic layout of the flat dilatometer test. (b) Seismic dilatometer equipment. (c) Schematic layout of the seismic dilatometer test (Marchetti *et al.*, 2001; Marchetti *et al.*, 2008).

C-reading, in sand, approximately equals the equilibrium pore pressure.

More detailed information on the DMT equipment, test procedure and all the interpretation formulae may be found in the comprehensive report by ISSMGE Technical Committee TC16 (Marchetti *et al.*, 2001).

3. Seismic Dilatometer Test (SDMT)

The seismic dilatometer (SDMT) is a combination of the mechanical flat dilatometer (DMT) with an add-on seismic module for measuring the shear wave velocity V_S. First introduced by Hepton (1988), the SDMT was subsequently improved at Georgia Tech, Atlanta, USA (Martin & Mayne, 1997, 1998; Mayne *et al.*, 1999). A new SDMT system (Figs. 1b and 1c) has been more recently developed in Italy (Marchetti *et al.*, 2008).

The seismic module (Fig. 1b) is a cylindrical element placed above the DMT blade, equipped with two receivers spaced at 0.50 m. The shear wave source, located at ground surface, is an automatic hammer or a pendulum hammer (≈ 10 kg) which hits horizontally a steel rectangular plate pressed vertically against the soil (by the weight of the truck) and oriented with its long axis parallel to the axis of the receivers, so that they can offer the highest sensitivity to the generated shear wave. When a shear wave is generated at the surface (Fig. 1c), it reaches first the upper receiver, then, after a delay, the lower receiver. The seismograms acquired by the two receivers, amplified and digitized at depth, are transmitted to a PC at the surface, which determines the delay. V_S is obtained as the ratio between the difference in distance between the source and the two receivers (S_2 - S_1) and the delay of the arrival of the impulse from the first to the second receiver (Δt).

The determination of the delay from SDMT seismograms, normally obtained using a cross-correlation algorithm rather than relying on the first arrival time or specific single points in the seismogram, is generally well conditioned. The *true-interval* test configuration with two receivers avoids possible inaccuracy in the determination of the "zero time" at the hammer impact, sometimes observed in the *pseudo-interval* one-receiver configuration. Moreover, the couple of seismograms recorded by the two receivers at a given test depth corresponds to the same hammer blow and not to different blows in sequence, which are not necessarily identical. Hence the repeatability of V_S measurements is considerably improved (observed V_S repeatability ≈ 1%, i.e. a few m/s). V_S measurements are taken every 0.50 m of depth (while the mechanical DMT readings are taken every 0.20 m). Validations of V_S measurements by SDMT by comparison with V_S measured by other *in situ* seismic tests at various research sites are reported by Marchetti *et al.* (2008).

4.Tentative Method for Deriving *in situ G*-γ Decay Curves from SDMT

Marchetti *et al.* (2008) first proposed the possible use of the SDMT for deriving *in situ* elemental soil stiffness variations with strain level (*G*-γ curves or similar). Such curves could be tentatively constructed by fitting "reference typical-shape" laboratory *G*-γ curves through two points, both obtained by SDMT: (1) the initial *small strain* modulus G_0 (obtained as $G_0 = \rho V_S^2$), and (2) a *working strain* modulus G_{DMT}.

To locate the second point on the *G*-γ curve it is necessary to know, at least approximately, the elemental shear strain corresponding to G_{DMT}. Indications by Mayne (2001) locate the DMT moduli at an intermediate level of strain (γ ≈ 0.05-0.1%) along the *G*-γ curve. Similarly Ishihara (2001) classified the DMT within the group of methods of measurement of soil deformation characteristics involving an intermediate level of strain (0.01-1%). The above qualitative indications are investigated in this paper.

As suggested by Marchetti *et al.* (2008), a *working strain shear modulus* G_{DMT} can be derived from the constrained modulus M_{DMT} provided by the usual DMT interpretation (Marchetti, 1980, Marchetti *et al.*, 2001). As a first approximation, by referring to linear elasticity:

$$G_{DMT} = \frac{1-2\nu}{2(1-\nu)} M_{DMT} \quad (1)$$

where ν = Poisson's ratio. E.g. assuming a typical drained ν of 0.2 (noting that M_{DMT} is a drained modulus), the *working strain shear modulus* may be obtained from Eq. 1 as G_{DMT} = 0.375 M_{DMT}. It should be noted that correlations between the DMT parameters (E_D and K_D) and M_{DMT} proposed by Marchetti (1980) are based on the assumption that M_{DMT} represents a reasonable estimate of the "operative" or drained *working strain* modulus (*i.e.* the modulus that, when introduced into the linear elasticity formulae, provides realistic estimates of the settlement of a shallow foundation under working loads). This assumption is supported by the good agreement observed in a large number of well documented comparisons between measured and DMT-predicted settlements or moduli (see Monaco *et al.*, 2006; Marchetti *et al.*, 2008).

The use of the SDMT to assess the *in situ* decay of stiffness at various test sites is explored in the following sections using data obtained in different soil types and where both SDMT data and "reference" stiffness decay curves were available. Such stiffness decay curves were: (a) back-figured from the observed behavior under a full-scale test embankment (Treporti) or footings (Texas), (b) obtained by laboratory tests (L'Aquila, Fucino plain, Po plain), or (c) reconstructed by the combined use of different *in situ*/laboratory techniques (Western Australia). The procedure adopted in all cases is as follows, and is shown schematically on Fig. 2:

1) Using SDMT data obtained at the same depth of each available reference stiffness decay curve, a *working strain* modulus G_{DMT} (or E_{DMT}) is derived from M_{DMT} and normalized by its *small strain* value G_0 (or E_0) derived from V_S.
2) The G_{DMT}/G_0 (or E_{DMT}/E_0) horizontal ordinate line is superimposed to the same-depth experimental stiffness decay curve, in such a way that the data point ordinate matches the curve;
3) The "intersection" of the G_{DMT}/G_0 (or E_{DMT}/E_0) horizontal ordinate line with the stiffness decay curve provides a shear strain value referred to here as γ_{DMT}.

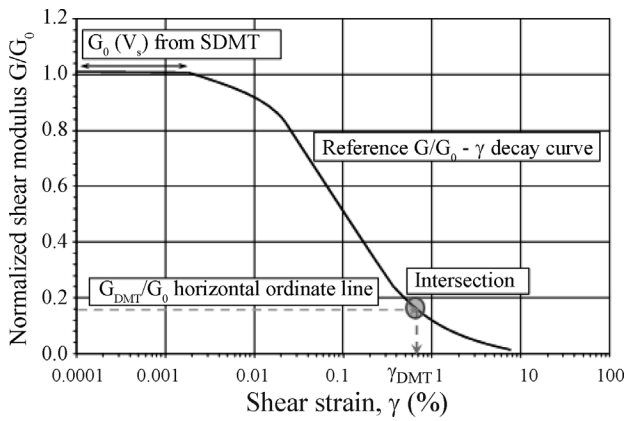

Figure 2 - Procedure to derive *in situ* G-γ decay curves from SDMT.

5. Stiffness Decay by SDMT at Various Test Sites

5.1. Treporti, Venice (Italy)

A full-scale vertically-walled cylindrical test embankment (40 m diameter, 6.7 m height, applied load 106 kPa) was constructed at the site of Treporti, Venice (Italy) where ground conditions are typical of the highly heterogeneous, predominantly silty deposits of the Venice lagoon. Pore pressures, surface settlements, horizontal movements and vertical displacements were monitored continuously and at various depths; see Simonini (2006). The Treporti test site was investigated extensively by means of piezocone tests (Gottardi & Tonni, 2004), flat dilatometer tests (Marchetti *et al.*, 2004), seismic piezocone tests and seismic dilatometer tests (McGillivray & Mayne, 2004), continuous coring boreholes and high quality laboratory tests (Simonini *et al.*, 2006). Significant results of the experimental program at Treporti have already been published by various research groups.

Figure 3 shows the profiles of the DMT parameters at Treporti, namely the material index I_D, the constrained modulus M_{DMT}, the undrained shear strength s_u and the horizontal stress index K_D from DMT 14 at the centre of the embankment, as well as the profiles of V_S obtained from SDMT 14 (McGillivray & Mayne, 2004), before starting the construction of the embankment (2002).

The Treporti embankment research has provided a unique opportunity to investigate the decay of soil stiffness *in situ* (Monaco *et al.*, 2014). Besides the moduli at the end of construction, moduli were also back-calculated in the elements on the centerline from local vertical strains ε_v measured during construction, under each load increment (from *small* to *working strains*). The stiffness considered in this section is the Young's modulus *E*.

In situ secant Young's moduli *E* were back-calculated at the mid-height of each 1 m soil layer as $E = (\Delta\sigma_v - 2\,\nu\,\Delta\sigma_r)/\varepsilon_v$, assuming vertical and radial stress increments $\Delta\sigma_v$ and $\Delta\sigma_r$ according to the theory of elasticity, ε_v obtained from extensometer data at the centre of the embankment under each load increment during construction (Marchetti *et al.*, 2006). Figure 4a shows the moduli corresponding to the first construction step (H = 0.5 m), to half-bank (H = 3.5 m) and to the construction end (H = 6.7 m). In the same figure, the small strain modulus E_0, derived from V_S

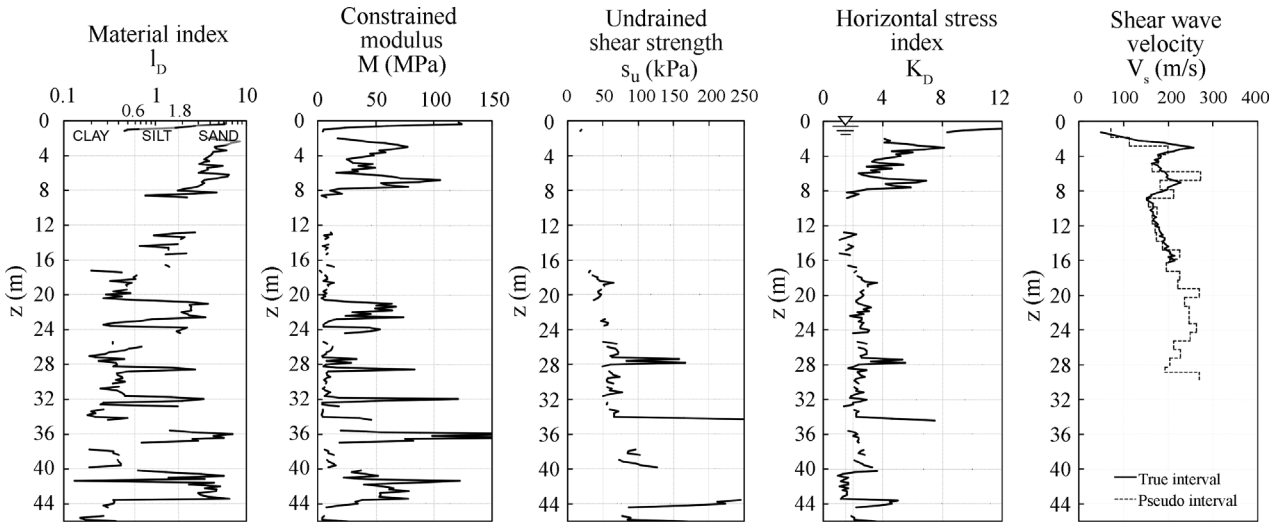

Figure 3 - Profiles of soil parameters from DMT 14 at the bank center (Marchetti *et al.*, 2004) and V_S profiles from SDMT 14 (McGillivray & Mayne, 2004) before embankment construction.

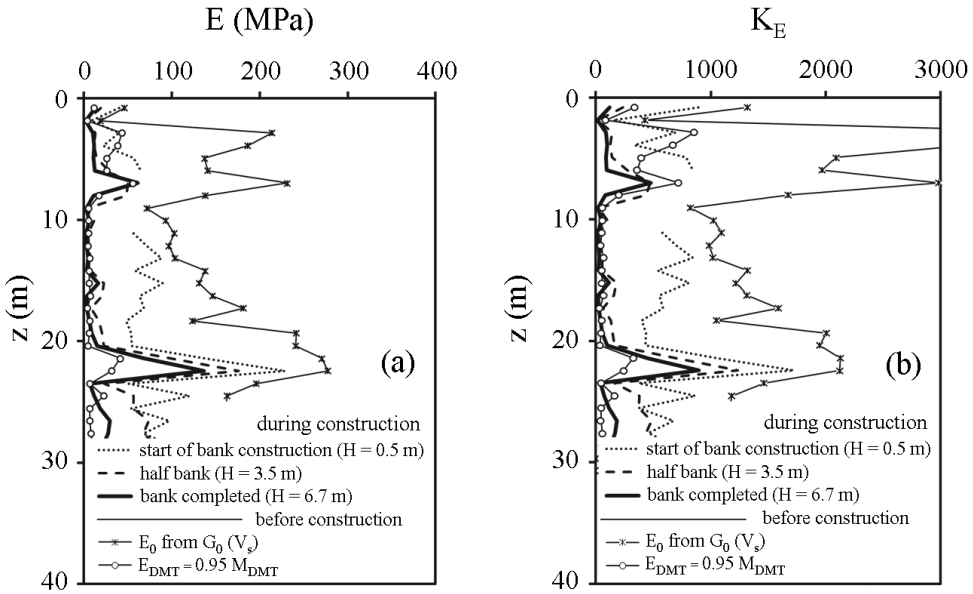

Figure 4 - Variation of (a) secant Young's modulus E, and (b) corresponding modulus number K_E (Eq. 2), back-calculated from local ε_v measured at the center under various embankment loads throughout construction (Monaco *et al.*, 2014, with permission from ASCE).

measured by SDMT, and the modulus E_{DMT} derived from M_{DMT} are shown for comparative purposes, assuming elasticity theory and a Poisson's ratio $\nu = 0.15$ for both cases (hence $E_{DMT} = 0.95\ M_{DMT}$). Figure 4a shows the progressive reduction of the back-calculated moduli E under increasing load. Such reduction should reflect the combined effects of the increase in stiffness with stress level and the reduction in stiffness with strain level.

In order to separate the two effects, the dependence of E on current stress level was taken into account, as a first approximation, by use of the Janbu's relation:

$$E = K_E\, p_a \left(\frac{\sigma'_v}{p_a} \right)^n \tag{2}$$

where K_E = modulus number, p_a = reference atmospheric pressure (100 kPa), σ'_v = current vertical effective stress, and n = exponent, generally varying between 0.5 to 1 and assumed here to equal 0.5, following the observations of Cola & Simonini (2002). The variation of the modulus number K_E in Eq. 2 corresponding to E back-calculated under each load increment is represented in Fig. 4b, which even more clearly shows the decay of stiffness, normalized for the effect of stress level, with increasing strain.

In situ decay curves of soil stiffness with strain level (Fig. 5) were reconstructed from the back-calculated moduli at the mid-height of each 1 m soil layer. To account for the effect of varying stress level, such *in situ* curves are expressed in terms of variation of the ratio K_E/K_{E0}, where K_E and K_{E0} are respectively the modulus number corresponding to E back-calculated for each load increment and to the initial modulus E_0 (K_{E0} is obtained by Eq. 2 for $E = E_0$ and $\sigma'_v = \sigma'_{v0}$). The two sets of curves in Fig. 5 are representative of two distinct soil layers: (a) the sand layer between 2 to 8 m depth, and (b) the low plasticity (plasticity index PI = 8-12%, Simonini *et al.*, 2006) silt layer between 8 to 20 m depth (which contributed most of the observed settlement). Note that the initial part of the curves in Fig. 5 at small strains is missing, since the extensometers did not provide reliable measurements of ε_v less than about 0.01-0.5%.

At Treporti test site, using SDMT results obtained at the depth of each back-figured *in situ* stiffness decay curve in Fig. 5, Young's moduli E_{DMT} were derived from M_{DMT} using elasticity theory and normalized by their small strain values E_0 derived from V_S. The E_{DMT} moduli were derived from the constrained moduli M_{DMT}, using the theory of elasticity, by Eq. 3:

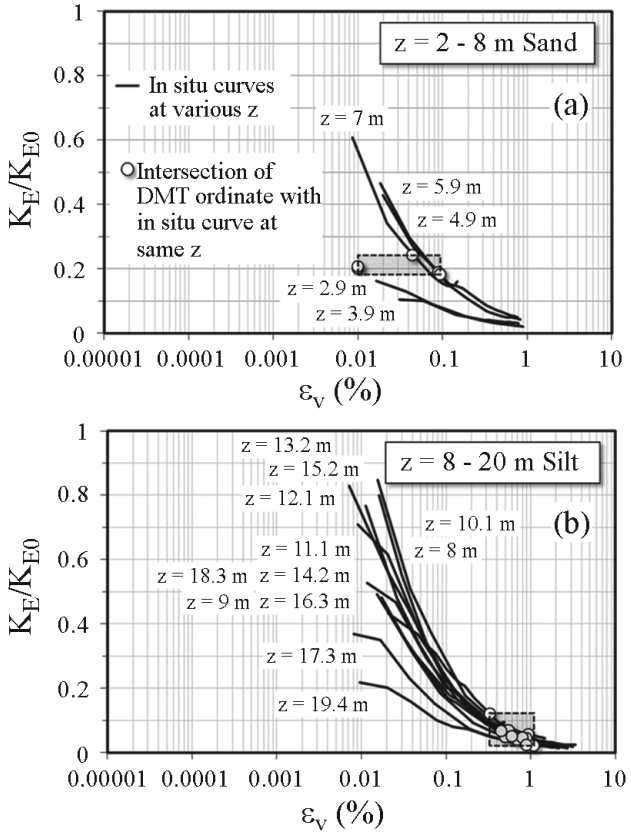

Figure 5 - Curves of decay of soil stiffness with vertical strain back-calculated from local ε_v measurements (curves labeled "*In situ* curves") in the sand layer 2 to 8 m depth (box a) and in the silt layer 8 to 20 m depth (box b). The dots are the intersection between the curve at a given depth and the horizontal line having as ordinate the ratio K_E/K_{E0} corresponding to E_{DMT}/E_0 at the same depth. Such "intersections" provided the values of the associated abscissas ε_v (Monaco *et al.*, 2014, with permission from ASCE).

$$E_{DMT} = \frac{M_{DMT}(1+\nu)(1-2\nu)}{(1-\nu)} \quad (3)$$

assuming $\nu = 0.15$, hence $E_{DMT} = 0.95\ M_{DMT}$.

The dots in Fig. 5 are the intersection between the *in situ* decay curve at a given depth and the horizontal line having as ordinate the ratio K_E/K_{E0} corresponding to E_{DMT}/E_0 at the same depth. Such "intersections" provided the values of the associated abscissas, i.e. the vertical strains ε_v in this case. The rectangular shaded areas in Figs. 5a and 5b denote, for each soil layer, the range of values of the ratio K_E/K_{E0} corresponding to E_{DMT}/E_0 and the associated range of vertical strains: $\varepsilon_v \approx 0.01$ to 0.1% in sand, ≈ 0.3 to 1% in silt (Monaco *et al.*, 2014).

Hence, the ratio G_{DMT}/G_0 was calculated by using the theory of elasticity (Eq. 4), while the corresponding shear strain γ_{DMT} was obtained by Eqs. 5, 6, as introduced by Atkinson (2000):

$$G_{DMT} = \frac{E_{DMT}}{2(1+\nu)} \quad (4)$$

assuming $\nu = 0.15$, hence $G_{DMT} = 0.43\ E_{DMT}$.

$$\varepsilon_s = (1+\nu)\varepsilon_v \quad (5)$$

$$\gamma_{DMT} = \frac{3}{2}\varepsilon_s \quad (6)$$

where ε_s = shear strain for the individual soil elements.

The values of the *normalized working strain shear modulus* G_{DMT}/G_0 range from 0.18 to 0.24 in sand and 0.02 to 0.12 in silt, while the range of values of the shear strain γ_{DMT} are 0.02% to 0.14% in sand, 0.50% to 1.65% in silt.

5.2. Texas A&M University National Geotechnical Experimentation Site (U.S.A.)

In 1994 a Spread Footing Prediction Symposium was conducted at the Texas A&M University National Geotechnical Experimentation Site, as part of the ASCE Geotechnical Specialty Conference Settlement '94. Five square footings, ranging in size from 1 to 3 m, were constructed and tested to obtain the complete load-settlement curves (Gibbens & Briaud, 1994a). The test site, composed of medium dense silty fine sand, was extensively investigated by several *in situ* tests (SPT, CPTU, DMT, borehole pressuremeter, Cross-Hole, borehole shear test and step blade test). Laboratory triaxial and resonant column tests were executed on reconstituted samples (Gibbens & Briaud, 1994b). Figure 6 plots the DMT profiles (DMT 1, DMT 2),

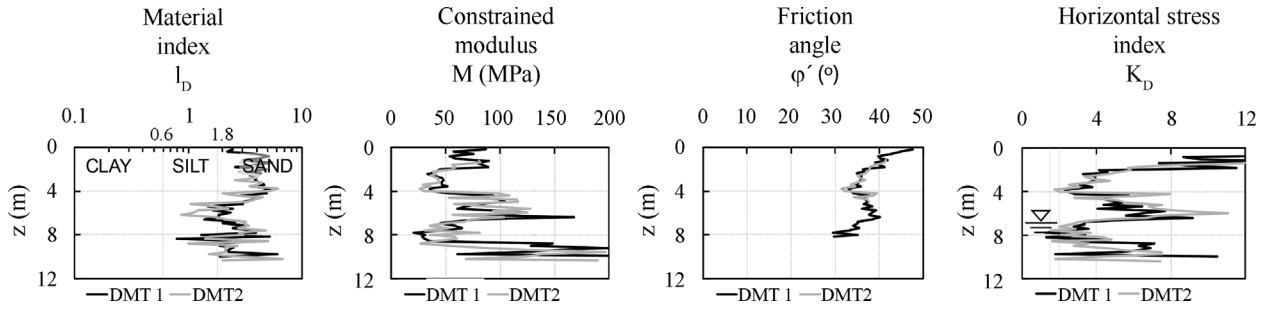

Figure 6 - DMT profiles at Texas A&M University National Geotechnical Experimentation Site (after Gibbens & Briaud, 1994b).

in terms of the material index I_D, the constrained modulus M, the friction angle φ' and the horizontal stress index K_D.

Figure 7 shows the *in situ* stiffness decay curve reconstructed by Berardi (1999) based on the observed performance of the footings. The Young's modulus E was backfigured from the observed load-settlement curves by use of a non linear iterative approach. The influence of current stress level was considered "implicit" in the E values determined over a limited influence depth, assumed within B and $2B$ (B = footing width). In Fig. 7 the decay of E, normalized to its initial value E_0, is plotted as a function of the relative displacement w/B% (footing settlement w/ width B).

From the results of two DMTs executed at the Texas A&M University test site, Young's moduli E_{DMT} (average values over an influence depth assumed within B and $2B$) were derived from M_{DMT} by Eq. 3, assuming ν = 0.2. The initial values of E_0 over the same depth interval were derived from V_S measured by Cross-Hole via elasticity theory (for ν = 0.2). In Fig. 7 the data points corresponding to E_{DMT}/E_0 for each footing size (3 m, 2 m, 1.5 m and 1 m) are superimposed to the E/E_0 - w/B curve reconstructed by Berardi (1999). The "intersection" of the DMT data points with the observed *in situ* decay curve indicates that the moduli estimated from DMT are located in a range of relative displacement $w/B \approx 0.25$ to 0.45%.

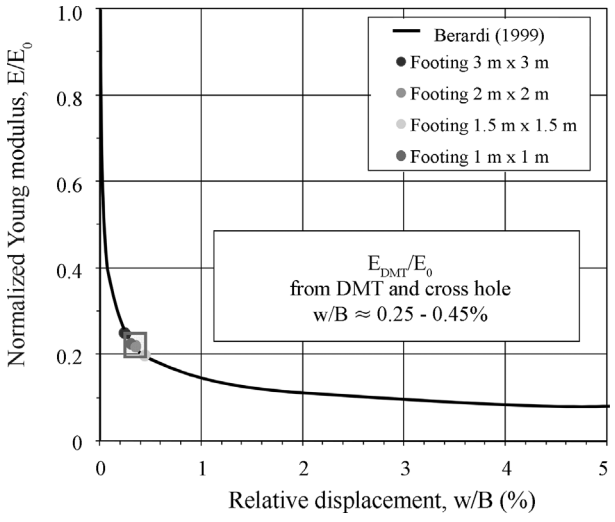

Figure 7 - Stiffness decay curve at Texas A&M University National Geotechnical Experimentation Site (Berardi, 1999) and superimposed E_{DMT}/E_0 data points (Amoroso *et al.*, 2012).

Hence, the ratio G_{DMT}/G_0 was calculated by using the theory of elasticity (Eq. 4), while the corresponding shear strain γ_{DMT} was obtained by Eqs. 6, 7, as introduced by Atkinson (2000):

$$\varepsilon_v \approx \frac{w}{3B} \tag{7}$$

The values of the *normalized working strain shear modulus* G_{DMT}/G_0 range from 0.20% to 0.25%, while the range of values of the shear strain γ_{DMT} are 0.02 to 0.14% in sand, 0.13 to 0.23% in silt.

5.3. L'Aquila (Italy)

Following the destructive April 6, 2009 earthquake (moment magnitude $M_w = 6.3$), the area of L'Aquila was extensively investigated by a variety of geotechnical and geophysical testing techniques, involving several working groups. Soon after the earthquake site investigations, including Down-Hole, surface wave tests and SDMT, were concentrated at a number of sites selected for the construction of new temporary houses for the homeless people (C.A.S.E. Project). Advanced cyclic/dynamic laboratory tests, including resonant column/torsional shear tests (RC-CTS) and double sample direct simple shear tests (DSDSS), were carried out on undisturbed samples from several C.A.S.E. sites, in medium- to fine-grained soils, by a network of Italian soil dynamics laboratories. Details and data are reported in Monaco *et al.* (2012); Santucci de Magistris *et al.* (2013); Monaco *et al.* (2013). The availability of both SDMT and laboratory test results at three C.A.S.E. sites (Cese di Preturo, Pianola, Roio Piano) permitted some calibration of empirical estimates of nonlinear parameters from SDMT (Amoroso *et al.*, 2012).

Coupled data from SDMT and resonant column/torsional shear tests were also obtained from an extensive geotechnical investigation performed in the Southern part of the city centre of L'Aquila for the reconstruction of several damaged buildings (Totani *et al.*, 2012; Amoroso *et al.*, 2015).

Table 1 reports the values of the shear wave velocity V_S measured by SDMT, the small strain shear modulus G_0 *in situ* obtained from V_S, the constrained modulus M_{DMT} obtained from the SDMT at the depth of the samples tested in the laboratory, the *working strain shear modulus* G_{DMT} calculated using Eq. 1, assuming ν = 0.2, and the plasticity index *PI*. The values of the *normalized working strain shear modulus* G_{DMT}/G_0, also reported in Table 1, result 0.10 to 0.23 in silt and clay, 0.37 in silty sand. Figure 8 plots the SDMT profiles, in terms of the material index I_D, the constrained modulus *M*, the undrained shear strength s_u, the horizontal stress index K_D and the shear wave velocity V_S at the four mentioned sites. In Fig. 9 each G_{DMT}/G_0 data point (grey symbols) is superimposed on the corresponding same-depth laboratory G/G_0 curve (RC tests by University of Napoli Federico II, DSDSS tests by University of Roma La Sapienza). The range of values of the shear strain γ_{DMT} resulting from the "intersection" of the G_{DMT}/G_0 data points with the laboratory curves (rectangular areas in Fig. 9) are γ_{DMT} = 0.24 to 0.52% in silt and clay, γ_{DMT} = 0.16% in silty sand; these are also reported in Table 1.

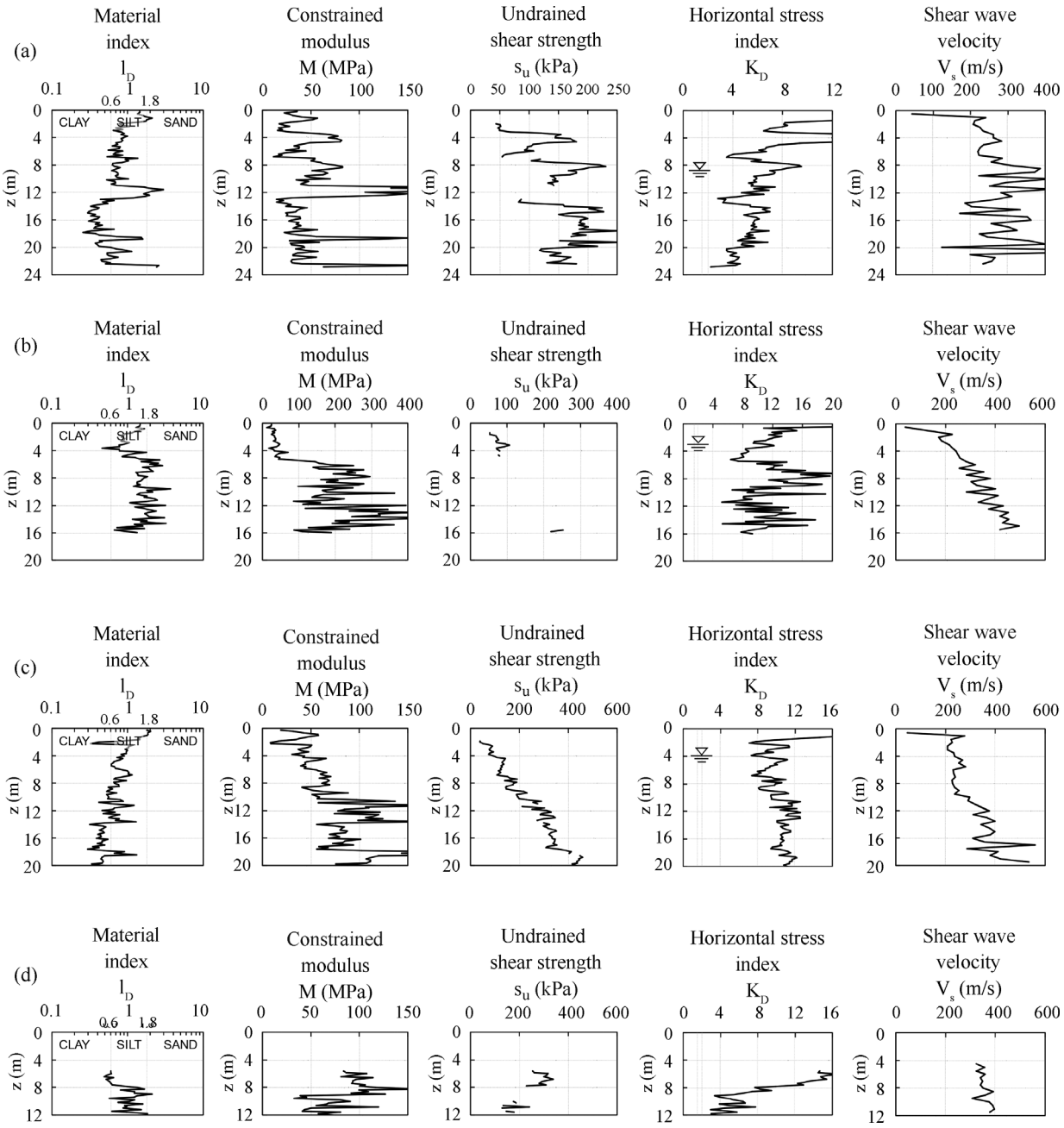

Figure 8 - SDMT profiles at L'Aquila basin: (a) Cese di Preturo, (b) Pianola, (c) Roio Piano, (d) L'Aquila (after Monaco *et al.*, 2012).

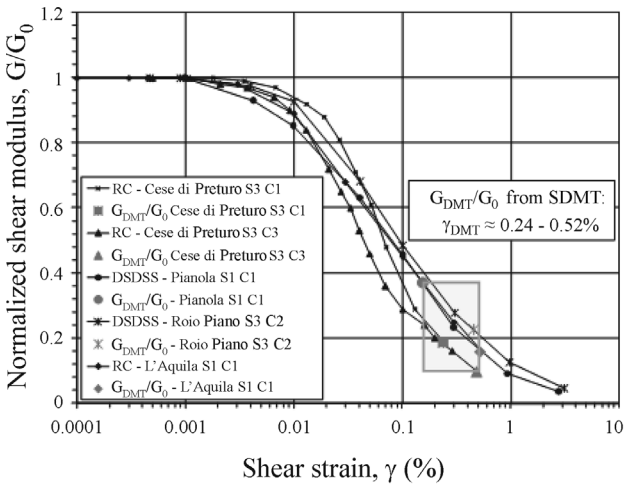

Figure 9 - Laboratory G/G_0-γ curves and superimposed G_{DMT}/G_0 data points at L'Aquila (after Amoroso *et al.*, 2012).

5.4. Fucino plain (Italy)

In 1986 a comprehensive investigation, involving static and dynamic loading effects, was carried out in the national research site of Fucino, Italy (Burghignoli *et al.*, 1991). *In situ* tests (SPT, CPT, DMT, self-boring pressumeter, vane test, Down-Hole, Cross-Hole, Spectral Analysis of Surface Waves) and laboratory tests (static and dynamic) were carried out to investigate the homogeneous lacustrine clay deposit to a depth of 40 m. Resonant column/torsional shear tests (RC-CTS) were executed on twelve undisturbed samples recovered from depths ranging between 3 and 37 m (effective vertical stress between 30 and 250 kPa). Although the data points pertain to a wide range of consolidation stresses, the results define, within a narrow band, the strong dependence of the stiffness on the strain level (Burghignoli *et al.*, 1991). In 2004 the same site in the Fucino plain was investigated by seismic dilatometer (Marchetti *et al.*, 2008) and the results are illustrated in Fig. 10.

Table 2 reports the values of the shear wave velocity V_S measured by SDMT, the small strain shear modulus G_0 *in situ* obtained from V_s, the constrained modulus M_{DMT} obtained by SDMT at the depth of the samples tested in the laboratory, the *working strain shear modulus* G_{DMT} calculated by Eq. 1, assuming $\nu = 0.2$, and the plasticity index *PI*. The values of the *normalized working strain shear modulus* G_{DMT}/G_0, also reported in Table 2, result 0.04 to 0.13 in clay. In Fig. 11 each G_{DMT}/G_0 data point (grey symbols) is superimposed on the corresponding same-depth laboratory G/G_0 curve (RC tests). The range of values of the shear strain γ_{DMT} resulting from the "intersection" of the G_{DMT}/G_0 data points with the laboratory curves (rectangular areas in Fig. 11) are γ_{DMT} = 1.10 to 1.70% in clay; these are also reported in Table 2.

Table 1 - L'Aquila - Values of G_{DMT}/G_0 obtained from SDMT and corresponding shear strain γ_{DMT} determined from the intersection with the G/G_0-γ laboratory curves (after Amoroso *et al.*, 2012).

Test site	Sample	Depth (m)	Soil type	V_S (m/s)	G_0 (MPa)	M_{DMT} (MPa)	ν	G_{DMT} (MPa)	G_{DMT}/G_0	γ_{DMT} (%)	PI (%)
Cese di Preturo	S3-C1	4.0-4.8	Silty clay	261	133	67	0.2	25	0.19	0.24	37
Cese di Preturo	S3-C3	17.5-18.0	Clayey silt	274	149	39	0.2	15	0.1	0.48	37
Pianola	S1-C1	6.0-6.5	Silty sand	303	195	193	0.2	72	0.37	0.16	31
Roio Piano	S3-C2	7.0-7.5	Clayey silt	233	105	64	0.2	24	0.23	0.46	19
L'Aquila	S1-C1	3.5-4.0	Clayey-sandy silt	344	232	97	0.2	36	0.16	0.52	31

Table 2 - Fucino plain - Values of G_{DMT}/G_0 obtained from SDMT and corresponding shear strain γ_{DMT} determined from the intersection with the G/G_0-γ laboratory curves.

Test site	Sample	Depth (m)	Soil type	V_S (m/s)	G_0 (MPa)	M_{DMT} (MPa)	ν	G_{DMT} (MPa)	G_{DMT}/G_0	γ_{DMT} (%)	PI (%)
Telespazio	-	5.0	Clay	70	14.7	1.4	0.2	0.5	0.04	1.70	30-70
Telespazio	-	10.0	Clay	101	15.7	1.8	0.2	0.7	0.04	1.70	30-70
Telespazio	-	15.0	Clay	98	17.7	2.2	0.2	0.8	0.05	1.60	30-70
Telespazio	-	20.0	Clay	124	16.7	4	0.2	1.5	0.09	1.40	30-70
Telespazio	-	25.0	Clay	156	16.7	5.6	0.2	2.1	0.13	1.10	30-70
Telespazio	-	30.0	Clay	183	17.7	5.9	0.2	2.2	0.13	1.10	30-70

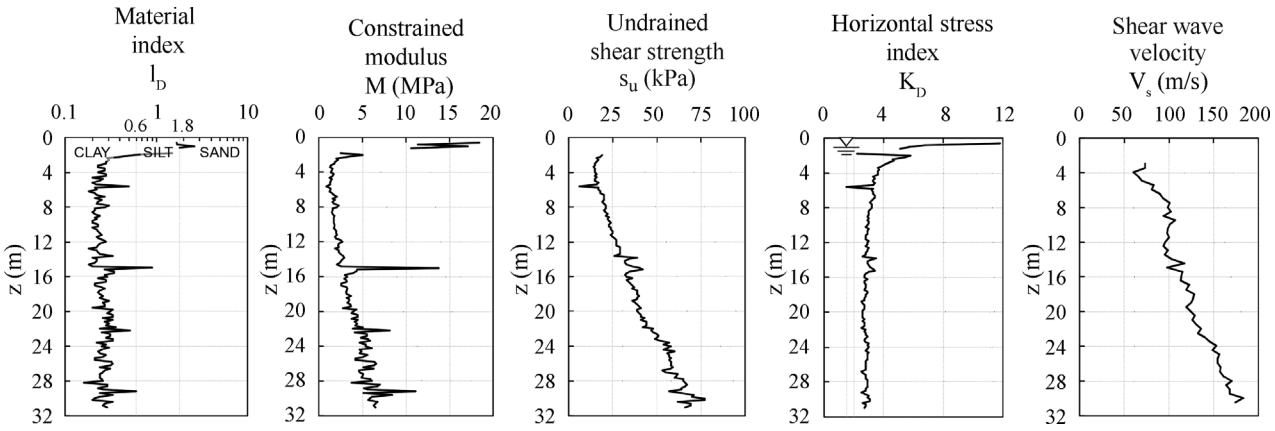

Figure 10 - SDMT profiles at Fucino plain (Marchetti *et al.*, 2008).

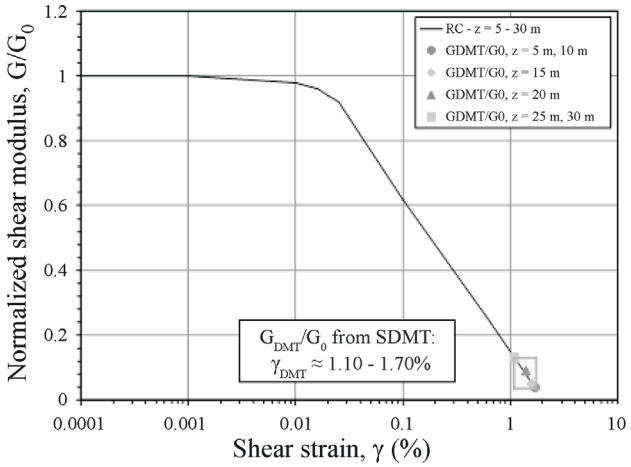

Figure 11 - Laboratory G/G_0-γ curve (Burghignoli *et al.*, 1991) and superimposed G_{DMT}/G_0 data points at Fucino plain.

5.5. Po plain (Italy)

The seismic sequence which affected northern Italy in May 2012, in particular the two main shocks that occurred on May 20, 2012 (M_w = 5.8) and May 29, 2012 (M_w = 5.6), induced several cases of liquefaction and related ground deformations.

An extensive site investigation program was subsequently planned by the "Liquefaction Working Group" promoted by the Emilia Romagna regional government and by the national Department of Civil Protection, in addition to the existing soil investigation data base, to characterize the soils and to define the input data necessary for site seismic response analyses and for assessment of liquefaction hazard (Regione Emilia Romagna - Liquefaction Working Group, 2012). The available results of this investigation programme, illustrated in various reports and papers (*e.g.* Facciorusso *et al.*, 2012, Fioravante *et al.*, 2013), include borehole logs, results of piezocone/seismic piezocone penetration tests (CPTU/SCPTU) and laboratory tests on samples, including resonant column/torsional shear tests (RC-CTS). An additional investigation involving seismic dilatometer (SDMTs), as illustrated in Fig. 12, as well as resonant column tests (RC) was carried out by the Working Group S2-UR4 (2013) and focused only on the area of San Carlo; see also Romeo *et al.* (2015). The town of San Carlo was constructed above the abandoned channel of the Reno River, and sand is the prevailing lithology in the band near this paleo-channel. Part of the town was built on the ancient banks of the Reno River.

The availability of results from both SDMT and laboratory resonant column (RC) tests on undisturbed samples taken in nearby boreholes in the area of San Carlo permitted some calibration of empirical estimates of non-linear parameters from SDMT.

Table 3 reports the values of the shear wave velocity V_S measured by SDMT, the small strain shear modulus G_0 *in situ* obtained from V_S, the constrained modulus M_{DMT} obtained from SDMTs performed at the depth of the samples tested in the laboratory, the *working strain shear modulus* G_{DMT} calculated by Eq. 1, assuming $\nu = 0.2$, and the plasticity index *PI*. The values of the *normalized working strain shear modulus* G_{DMT}/G_0 range from 0.07 to 0.10 in silt and clay, and 0.06 to 0.32 in silty sand; see Table 3. In Fig. 13 each G_{DMT}/G_0 data point (black and grey symbols) is superimposed on the corresponding same-depth laboratory G/G_0 curve (RC tests). The range of values of the shear strain γ_{DMT} resulting from the "intersection" of the G_{DMT}/G_0 data points with the laboratory curves (rectangular areas in Fig. 13) are γ_{DMT} = 0.32% to 0.47% in silt and clay, γ_{DMT} = 0.07 to 0.30% in silty sand; see Table 3.

5.6. Western Australia

The G/G_0-γ decay curves presented in this section were obtained at five different test sites in Western Australia (Shenton Park, Ledge Point, Perth CBD, East Perth, Margaret River). Such curves were constructed based on the results of several *in situ* tests, including flat/seismic dilatometer tests (DMT/SDMT), seismic cone penetration tests (SCPT), self-boring pressuremeter tests (SBP) and

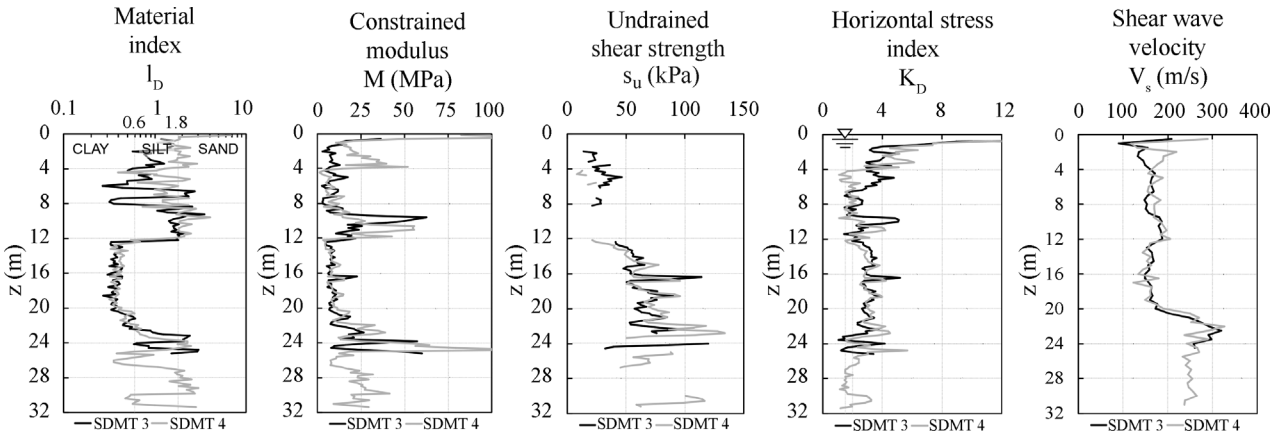

Figure 12 - SDMT profiles at Po plain (Working Group S2-UR4, 2013).

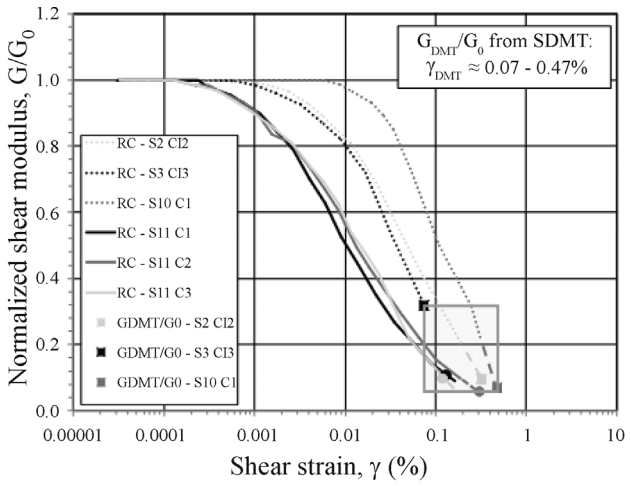

Figure 13 - Laboratory G/G_0-γ curves (after Fioravante *et al.*, 2013) and superimposed G_{DMT}/G_0 data points at Po plain.

laboratory triaxial tests. Details can be found in Amoroso (2011), Fahey *et al.* (2003, 2007), Lehane *et al.* (2007), Lehane (2010), Lehane & Fahey (2004), Schneider *et al.* (2008), Schneider & Lehane (2010).

Figure 14 shows the SDMT profiles, in terms of the material index I_D, the constrained modulus M_{DMT}, the inferred friction angle φ' or the undrained shear strength s_u, the horizontal stress index K_D and the shear wave velocity V_S at the three mentioned sites.

The *in situ* normalized G/G_0-γ decay curves shown in Fig. 15 (Shenton Park, silica sand), Fig. 16 (Ledge Point, calcareous sand) and Fig. 17 (Perth CBD, alluvial silty clay) were reconstructed by combining the information resulting from SCPT and SBP. In particular:

- the initial part of the curves ($\gamma \leq 0.001\%$) was characterized by the small strain shear modulus G_0 obtained from V_S measured by SCPT (no SDMT data were available at these sites);
- the non-linear G/G_0-γ decay at medium to large shear strains ($\gamma \geq 0.01\%$) was estimated based on SBP data, according to the procedure proposed by Jardine (1992);
- the central part of the curves ($0.001\% > \gamma > 0.01\%$) was defined by simply connecting the initial part obtained from SCPT (G_0) and the final part obtained from SBP.

The *working strain shear modulus* G_{DMT} was calculated from M_{DMT} obtained by DMT at the same depths of the SCPT and SBP data used to define the G/G_0-γ curve, by use of Eq. 1, assuming $\nu = 0.2$ in sand in silty clay. The values

Table 3 - Po plain - Values of G_{DMT}/G_0 obtained from SDMT and corresponding shear strain γ_{DMT} determined from the intersection with the G/G_0-γ laboratory curves (after Working Group S2-UR4, 2013).

Test site	Sample	Depth (m)	Soil type	V_S (m/s)	G_0 (MPa)	M_{DMT} (MPa)	ν	G_{DMT} (MPa)	G_{DMT}/G_0	γ_{DMT} (%)	PI (%)
San Carlo	S3 CI3	9.5-9.6	Silty sand	181	64	54	0.2	20	0.32	0.07	-
San Carlo	S10 CI1	13-13.6	Silty clay	159	46	8	0.2	3	0.07	0.47	49
San Carlo	S2 CI2	7.3-7.4	Sandy silt	175	53	14	0.2	5	0.10	0.32	12-17
San Carlo	S11 CI1	2.0-2.6	Silty sand	205	75	23	0.2	9	0.11	0.13	-
San Carlo	S11 CI2	6.0-6.6	Silty sand	157	42	7	0.2	3	0.06	0.30	-
San Carlo	S11 CI3	9.0-9.6	Silty sand	170	53	14	0.2	5	0.10	0.12	-

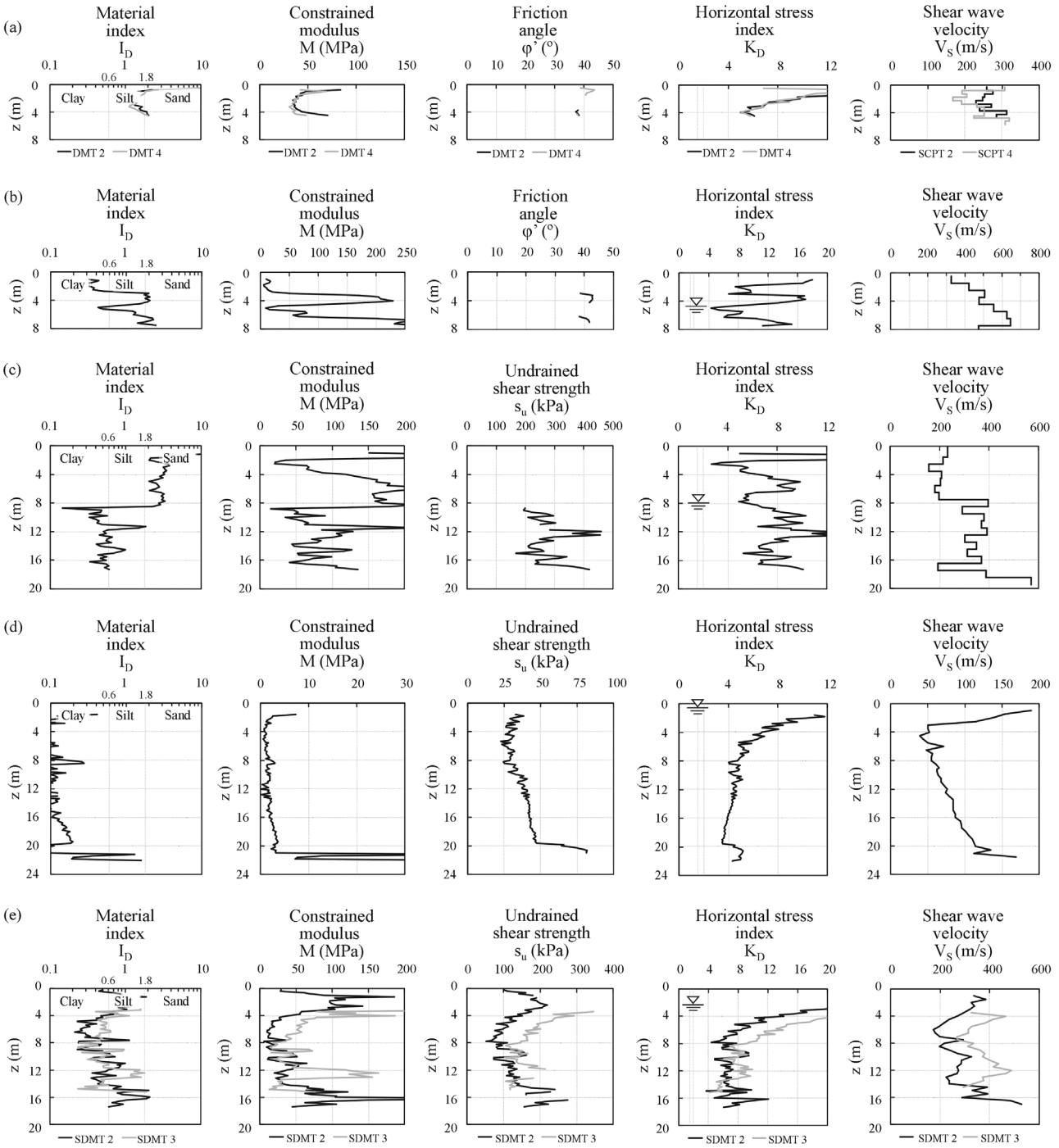

Figure 14 - DMT profiles and V_S profiles at different sites in Western Australia: (a) Shenton Park, (b) Ledge Point, (c) Perth CBD, (d) East Perth, (e) Margaret River (Amoroso, 2011).

of G_{DMT}/G_0 range from 0.10 to 0.20 in silica sand, 0.08 to 0.31 in calcareous sand, 0.09 to 0.30 in silty clay; see Table 4. The black and grey symbols in Figs. 15, 16 and 17 represent the position of the G_{DMT}/G_0 data points on the corresponding *in situ* reference G/G_0-γ decay curves. The range of values of the shear strain γ_{DMT} resulting from the "intersection" with the *in situ* G/G_0-γ curves (rectangular shaded areas in Figs. 15, 16 and 17), also reported in Table 4, are γ_{DMT} = 0.04-0.15% in sand and γ_{DMT} = 0.23-1.50% in silty clay.

The G/G_0-γ decay curves shown in Fig. 18 (East Perth, soft clay) and Fig. 19 (Margaret River, silty clay) were reconstructed by combining the information resulting

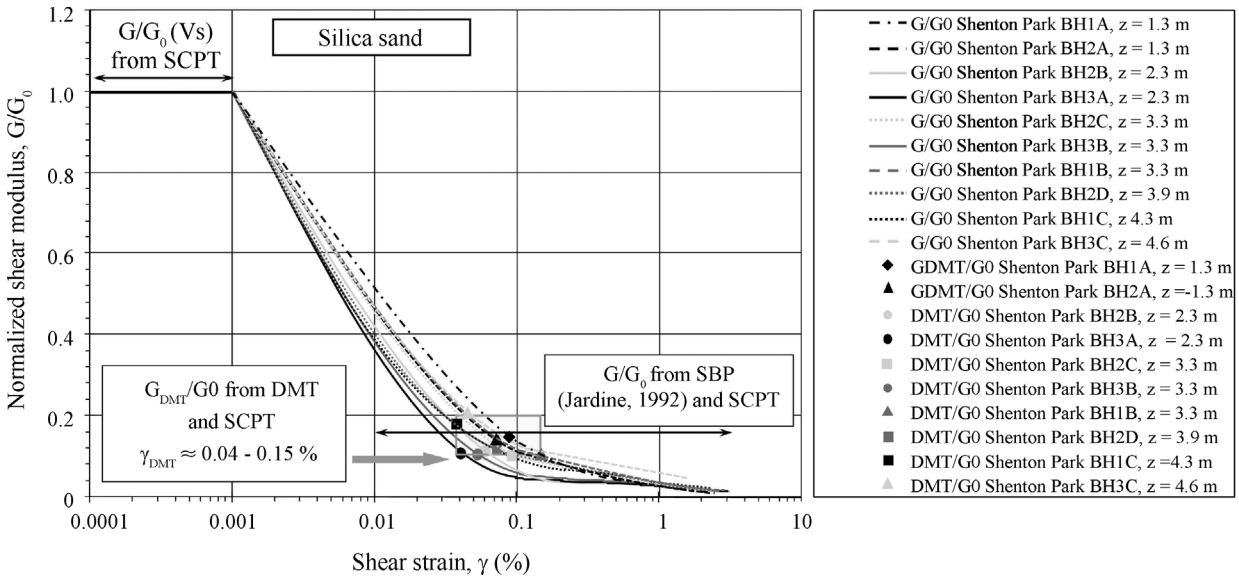

Figure 15 - *In situ* G/G_0-γ decay curves and superimposed G_{DMT}/G_0 data points at Shenton Park (silica sand), Western Australia (Amoroso *et al.*, 2012).

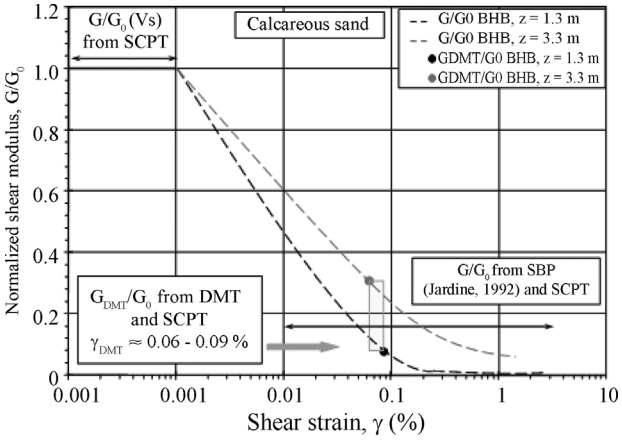

Figure 16 - *In situ* G/G_0-γ decay curves and superimposed G_{DMT}/G_0 data points at Ledge Point (calcareous sand), Western Australia (Amoroso *et al.*, 2012).

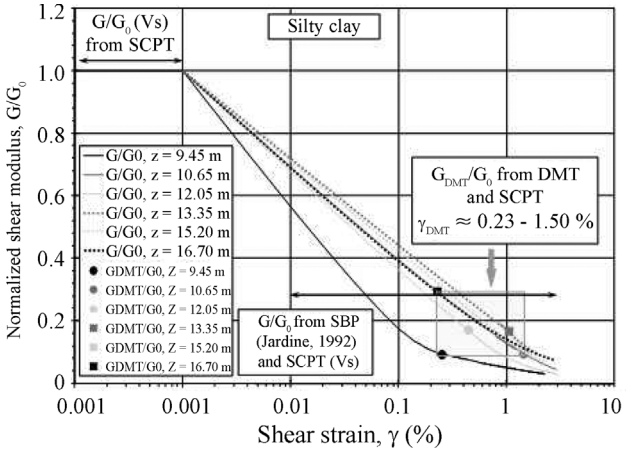

Figure 17 - *In situ* G/G_0-γ decay curves and superimposed G_{DMT}/G_0 data points at Perth CBD (silty clay), Western Australia (after Amoroso *et al.*, 2012).

from *in situ* SDMT and laboratory triaxial tests. In this case:

- the initial part of the curves ($\gamma \leq 0.001\%$) was characterized by G_0 derived from V_S measured by SDMT;
- the non-linear G/G_0-γ decay at medium to large shear strains ($\gamma \geq 0.1\%$ at Margaret River, $\gamma \geq 0.5\%$ at East Perth) was estimated from triaxial tests according to Atkinson (2000);
- the central part of the curves ($0.001\% > \gamma > 0.5\%$ at East Perth, $0.001\% > \gamma > 0.1\%$ at Margaret River) was defined by simply connecting the initial part obtained from SDMT (G_0) and the final part obtained from triaxial tests.

The *working strain shear modulus* G_{DMT} was calculated from M_{DMT} obtained by SDMT at the same depths of the samples tested in the laboratory by use of Eq. 1, assuming $\nu = 0.2$ at both sites. The values of G_{DMT}/G_0 vary from 0.04 in soft clay to 0.07 in silty clay; see Table 4. The values of the shear strain γ_{DMT} resulting from the "intersection" of the G_{DMT}/G_0 data points with the reconstructed reference G/G_0-γ decay curves (dot symbols in Figs. 18 and 19) are 5.5% in soft clay and vary from 0.23% to 1.50% in silty clay; see Table 4.

6. Discussion

6.1. Summary of results at various test sites

Over the past decades, numerous studies have been conducted regarding the dynamic soil properties and the

Table 4 - Western Australia - Values of G_{DMT}/G_0 obtained from SDMT (or DMT + SCPT) and corresponding shear strain γ_{DMT} determined from the intersection with the G/G_0 - γ reference curves at five test sites (Amoroso *et al.*, 2012).

Test site	Sample	Depth (m)	Soil type	V_S (m/s)	G_0 (MPa)	M_{DMT} (MPa)	ν	G_{DMT} (MPa)	G_{DMT}/G_0	γ_{DMT} (%)	PI (%)
Shenton Park	BH1A	1.3	Silica sand	252	105	42	0.2	16	0.15	0.09	-
Shenton Park	BH2A	1.3	Silica sand	252	105	40	0.2	15	0.14	0.07	-
Shenton Park	BH2B	2.3	Silica sand	267	118	35	0.2	13	0.11	0.06	-
Shenton Park	BH3A	2.3	Silica sand	267	118	33	0.2	12	0.11	0.04	-
Shenton Park	BH2C	3.3	Silica sand	280	129	36	0.2	14	0.11	0.15	-
Shenton Park	BH3B	3.3	Silica sand	280	129	36	0.2	13	0.10	0.09	-
Shenton Park	BH1B	3.3	Silica sand	280	129	35	0.2	13	0.10	0.05	-
Shenton Park	BH2D	3.9	Silica sand	282	132	42	0.2	16	0.12	0.07	-
Shenton Park	BH1C	4.3	Silica sand	283	132	63	0.2	23	0.17	0.04	-
Shenton Park	BH3C	4.6	Silica sand	283	132	72	0.2	27	0.20	0.05	-
Ledge Point	BHB	1.3	Calcareous sand	217	78	16	0.2	6	0.08	0.09	-
Ledge Point	BHB	3.3	Calcareous sand	361	215	176	0.2	76	0.31	0.06	-
Perth CBD	NML4	9.45	Silty clay	334	212	52	0.2	20	0.09	0.25	20
Perth CBD	NML4	10.65	Silty clay	373	264	67	0.2	25	0.10	1.45	20
Perth CBD	NML4	12.05	Silty clay	388	286	130	0.2	49	0.17	0.45	20
Perth CBD	NML4	13.35	Silty clay	319	193	86	0.2	32	0.17	1.05	20
Perth CBD	NML4	15.2	Silty clay	324	199	56	0.2	21	0.11	1.5	20
Perth CBD	NML4	16.7	Silty clay	260	128	101	0.2	38	0.30	0.23	20
East Perth	BH6	15.8-16.0	Soft clay	87	12	1.8	0.2	0.5	0.04	5.5	45-50
Margaret R.	BH3	6.0	Silty clay	174	55	13	0.2	4	0.07	1.75	43
Margaret R.	BH5	9.0	Silty clay	362	256	68	0.2	20	0.07	0.36	13

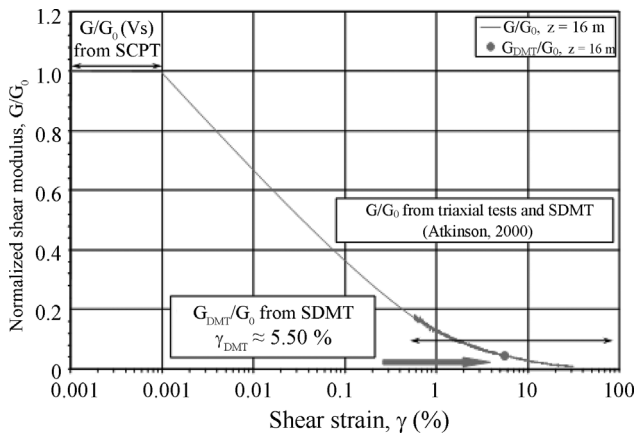

Figure 18 - *In situ* G/G_0-γ decay curves and superimposed G_{DMT}/G_0 data points at East Perth (soft clay), Western Australia (Amoroso *et al.*, 2012).

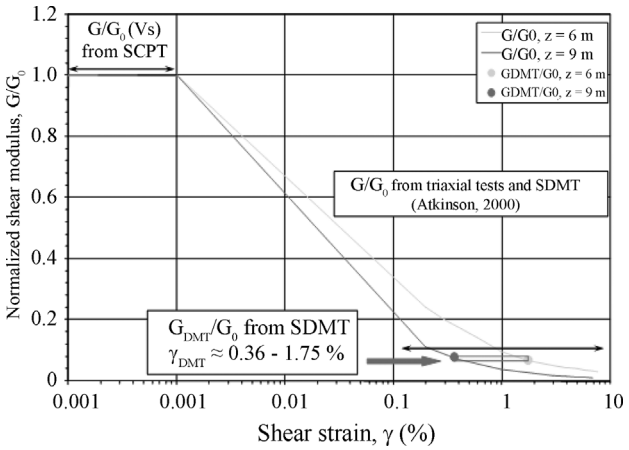

Figure 19 - *In situ* G/G_0-γ decay curves and superimposed G_{DMT}/G_0 data points at Margaret River (silty clay), Western Australia (Amoroso *et al.*, 2012).

parameters affecting them, such as the mean effective confining pressure, the soil type and the plasticity. Various investigators have proposed non linear curves for sands (for example Darendeli, 2001; Seed *et al.*, 1986; Iwasaki *et al.*, 1978; Kokusho, 1980), clays and silts with different plasticity (for example Darendeli 2001; Vucetic & Dobry, 1991; Sun *et al.*, 1988). Figure 20 summarizes the upper and lower ranges of these typical curves, obtained for different values of the mean effective confining pressure, assumed between 25 and 1600 kPa, and a plasticity index *PI* ranging between 0% and 100%. Figure 20 shows that the curves proposed by Darendeli (2001) including all the other reference curves.

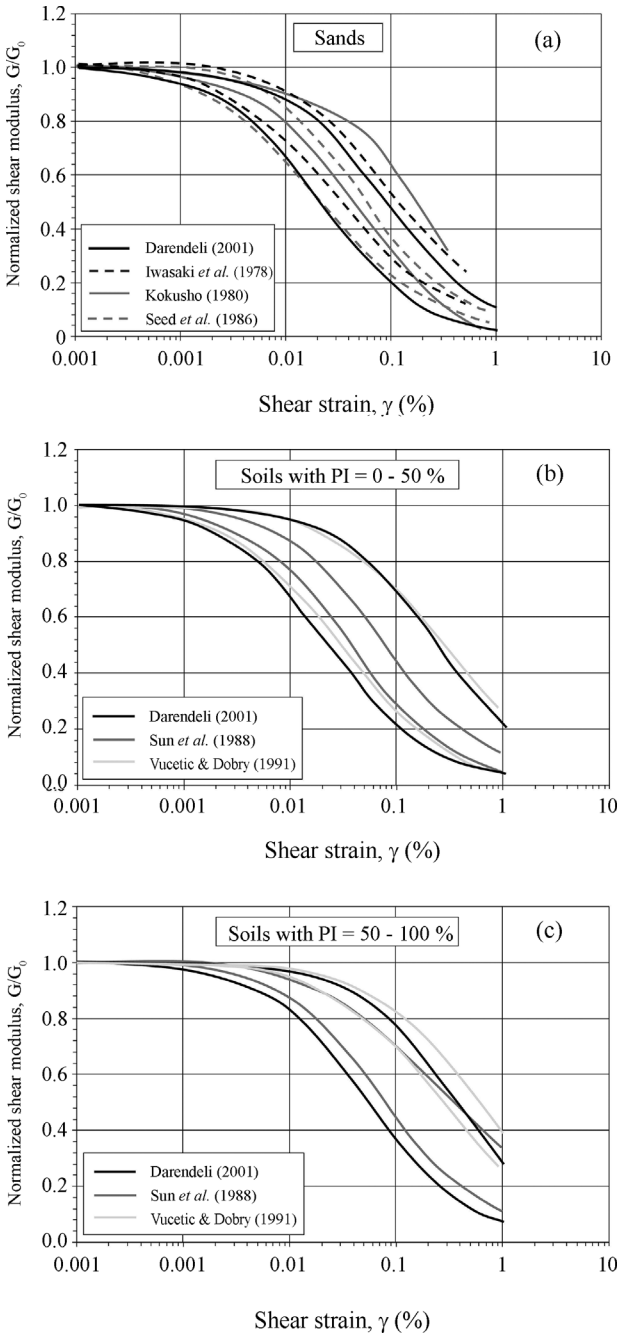

Figure 20 - Reference G/G_0-γ decay curves: (a) sands, (b) silts and clays with plasticity index *PI* = 0-50%, (c) silts and clays with plasticity index *PI* = 50-100%.

Figure 21 depicts the possible use of the SDMT for calibrating the selection of *in situ* G/G_0-γ decay curves in various soil types. The results obtained at all the test sites previously described were superimposed on the Darendeli (2001) G/G_0-γ stiffness decay curves. The rectangular shaded areas in Fig. 21 represent the range of values of the *normalized working strain shear modulus* G_{DMT}/G_0 determined in different soil types (sand, silt and clay) and the corresponding shear strain γ_{DMT} determined by the "intersection" procedure. Based on the available information, the "typical range" of shear strain associated to the working strain moduli G_{DMT} can be approximately assumed as: $\gamma_{DMT} \approx$ 0.01-0.45% in sand, $\gamma_{DMT} \approx$ 0.1-1.9% in silt and clay. In soft clay the values of $\gamma_{DMT} > 2\%$ (not shown in Fig. 21) are too high to attempt an interpolation using a reference stiffness decay curve.

These observations are in agreement with preliminary literature indications (Mayne, 2001; Ishihara, 2001). Moreover, the calculated values of the ratio G_{DMT}/G_0 - which could be regarded as the shear modulus decay factor at *working strains* - are in line with the trends observed by Marchetti *et al.* (2008), who investigated the experimental interrelationship between *small strain* and *working strain* stiffness using SDMT in sand, silt and clay. In particular, the diagrams of the ratio G_{DMT}/G_0 vs. the DMT horizontal stress index K_D (related to OCR) constructed by Marchetti *et al.* (2008) using the SDMT results at 34 different sites, in a variety of soil types, indicated that the *G* decay in sands is more significant at lower strains than in silts and clays, and that the decay curves in silts and clays are very similar.

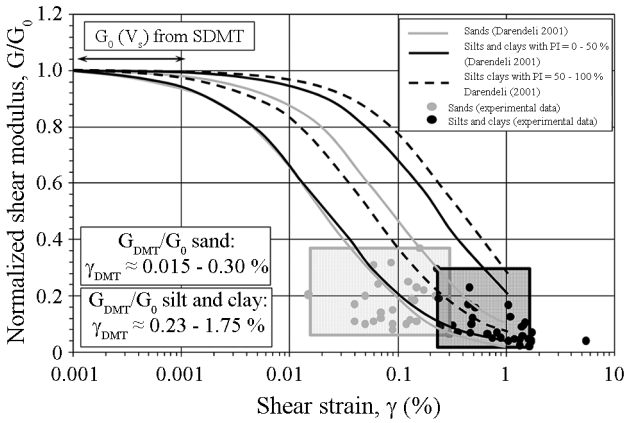

Figure 21 - Possible use of the SDMT for calibrating the selection of *in situ* G/G_0-γ decay curves in various soil types.

6.2. Proposed numerical G-γ decay curves from SDMT

Several authors (Hardin & Drnevich, 1972; Bellotti *et al.*, 1989; Byrne *et al.*, 1990; Fahey & Carter, 1993; Fahey, 1998) introduced a hyperbolic model to represent the non-linear stress-strain behaviour of soil in pressuremeter tests. In this respect, the SDMT experimental data determined at all the investigated test sites (Fig. 22) were used to assist the construction of a hyperbolic stress-strain equation (Eq. 8):

$$\frac{G}{G_0} = \frac{1}{1+\left(\frac{G_0}{G_{DMT}}-1\right)\frac{\gamma}{\gamma_{DMT}}} \quad (8)$$

Thus, the ratio G_{DMT}/G_0 obtained from SDMT and the estimated shear strain γ_{DMT} were used to plot the corresponding hyperbolic curve at each test site. In the examples shown in Fig. 23a (Shenton Park, sand) and 23b (Roio Piano, clayey silt), the curves obtained from SDMT, using Eq. 8 and the coupled values of G_{DMT}/G_0 - γ_{DMT} introduced in the tables (thick black lines in Figs. 23a and b), evidently provide a reasonable fit to the "measured" stiffness decay curves.

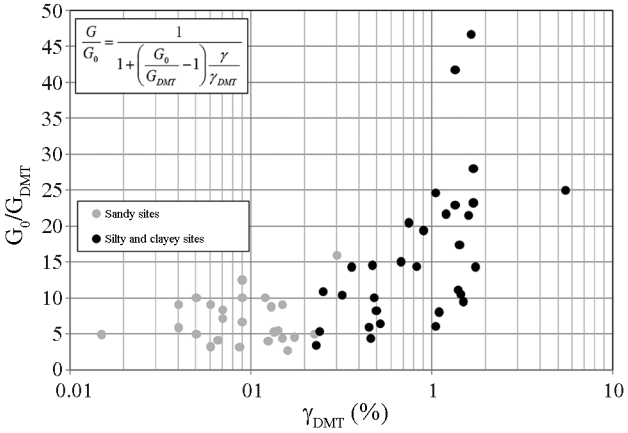

Figure 22 - SDMT experimental data used to assist the construction of a hyperbolic equation.

The estimated γ_{DMT} values for each case history examined are plotted on Fig. 23. It is apparent that γ_{DMT} values in clays are higher than those in sands; this trend is in keeping with that seen on Fig. 20. Combined with a measured G_{DMT}/G_0 value from the SDMT, Fig. 23 can be used in combination with Eq. 8 to provide a first order estimate of a given soil's elemental G vs γ curve. It is noted that hyper-

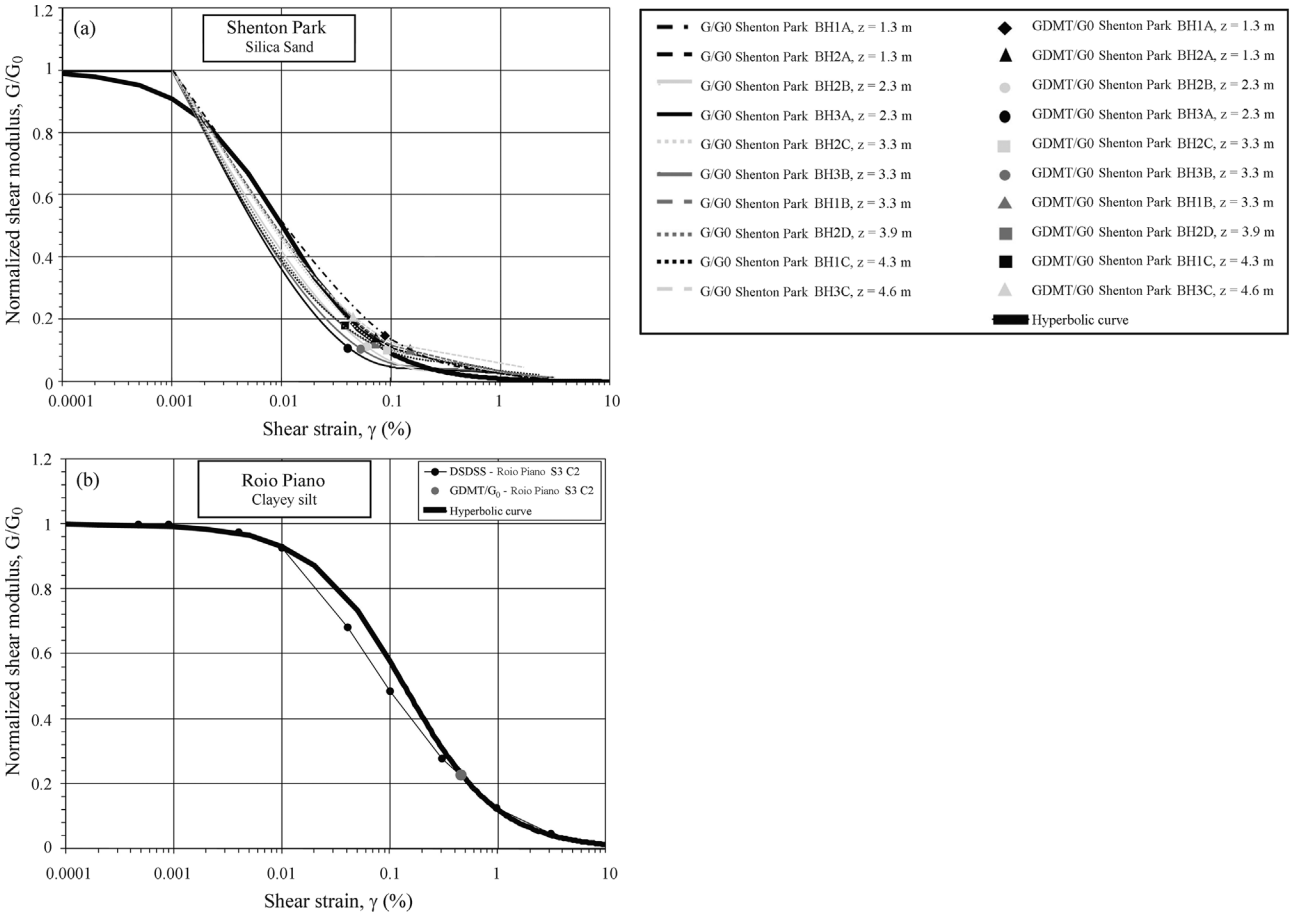

Figure 23 - Comparison between hyperbolic and "measured" stiffness decay curves at Shenton Park (a) and Roio Piano (b).

bolic G vs γ curves have been seen to be particularly relevant for dynamic/cyclic applications.

7. Conclusions

The results presented in this paper support the possible use of the SDMT to assess the decay of *in situ* stiffness with strain level and to address the selection of elemental G-γ curves in various soil types. This potential stems from the ability of the SDMT to provide routinely, at each test depth, both a *small strain* stiffness (G_0 from V_S) and a *working strain* stiffness G_{DMT} (derived via standard DMT correlations). "Reference typical-shape" laboratory G-γ curves may be tentatively fitted through these two stiffness values. A significant premise of this approach is that, to locate the second point on the G-γ curve, it is necessary to know (at least approximately) the shear strain γ_{DMT} corresponding to *working strain modulus* G_{DMT}.

Typical ranges of γ_{DMT} in different soil types have been inferred from the "intersection" of the SDMT data points with same-depth reference stiffness decay curves - backfigured from the observed field behavior under full-scale loading, or obtained by cyclic/dynamic laboratory tests or reconstructed by the combined use of different *in situ*/laboratory techniques - at various test sites.

Based on the available information, γ_{DMT} is typically about 0.1% in sand, about 0.5 to 1.0% in silt and clay and greater than 2% in soft clay. The proposed hyperbolic relationship, together with an estimate of γ_{DMT} from Fig. 21, can provide a useful first order estimate of a soil's G-γ degradation curve.

Acknowledgments

Special thanks to Prof. Silvano Marchetti for providing the initial ideas for this study, and for his precious and continuous suggestions to support this research. Special thanks also to Prof. Martin Fahey for offering his knowledge and experience to critically approach the present study.

References

Amoroso, S. (2011) G-γ decay curves by seismic dilatometer (SDMT). PhD Dissertation, Department of Structural, Water and Soil Engineering, University of L'Aquila, L'Aquila, 480 p.

Amoroso, S.; Monaco, P. & Marchetti, D. (2012) Use of the Seismic Dilatometer (SDMT) to estimate *in situ* G-γ decay curves in various soil types. Coutinho, R. & Mayne, P.W. (eds) Proc. 4th Int. Conf. on Geotechnical and Geophysical Site Characterization, ISC'4, Porto de Galinhas, Brazil, v. 1, p. 489-497.

Amoroso, S.; Totani, F.; Totani, G. & Monaco, P. (2015) Local seismic response in the Southern part of the historic centre of L'Aquila. Engineering Geology for Society and Territory - Urban Geology, Sustainable Planning and Landscape Exploitation, Springer International Publishing, v. 5:XVIII, p. 1097-1100.

Atkinson, J.H. (2000) Non-linear soil stiffness in routine design. Géotechnique, v. 50:5, p. 487-508.

Bellotti, R.; Ghionna, V.; Jamiolkowski, M.; Robertson, P.K. & Peterson, R.W. (1989) Interpretation of moduli from self-boring pressumeter tests in sand. Géotechnique, v. 39, p. 269-292.

Berardi, R. (1999) Non linear elastic approaches in foundation design. Jamiolkowski, M.; Lancellotta R. & Lo Presti D.C.F. (eds) Pre-Failure Deformation Characteristics in Geomaterials. Balkema, Rotterdam, p. 733-739.

Burghignoli, A.; Cavalera, L.; Chieppa, V.; Jamiolkowski, M.; Mancuso, C.; Marchetti, S.; Pane, V.; Paoliani, P.; Silvestri, F.; Vinale, F. & Vittori, E. (1991) Geotechnical characterization of Fucino clay. Proc. X ECSMFE, Firenze, v. 1, p. 27-40.

Byrne, P.M.; Salgado, F.M. & Howie, J.A. (1990) Relationship between the unload shear modulus from pressumeter tests and the maximum shear modulus for sands. Proc. 3rd International Symposium on Pressumeters, ISP3, Oxford, p. 231-241.

Cola, S. & Simonini, P. (2002) Mechanical behaviour of silty soils of the Venice lagoon as a function of their grading properties. Can. Geotech. J., v. 39:4, p. 879-893.

Darendeli, M.B. (2001) Development of a New Family of Normalized Modulus Reduction and Material Damping Curves. PhD Dissertation, University of Texas.

Elhakim, A.F. & Mayne, P.W. (2003) Derived stress-strain-strength of clays from seismic cone tests. Proc. 3rd Int. Symp. Deform. Charact. Geomaterials, Lyon, v. 1, p. 81-87.

Facciorusso, J.; Madiai, C. & Vannucchi, G. (2012) Risposta sismica locale e pericolosità sismica di liquefazione a San Carlo e Mirabello (FE). University of Florence, 3 October 2012 (in Italian), http://ambiente.regione.emilia-romagna.it/geologia/temi/sismica/liquefazione-gruppo-di-lavoro/RAPPORTO_RSL_LIQ_ott_2012_UNIFI.pdf/at_download/file/RAPPORTO_RSL_LIQ_ott_2012_UNIFI.pdf.

Fahey, M. & Carter, J.P. (1993) A finite element study of the pressuremeter test in sand using a non-linear elastic plastic model. Can. Geotech. J., v. 30, p. 348-362.

Fahey, M. (1998) Deformation and *in situ* stress measurement. Robertson P.K. & Mayne P.W. (eds) Proc. 1st Int. Conf. on Site Characterization, Atlanta, v. 1, p. 49-68.

Fahey, M.; Lehane, B.M. & Stewart, D. (2003) Soil stiffness for shallow foundation design in the Perth CBD. Australian Geomechanics, v. 38:3, p. 61-90.

Fahey M.; Schneider, J.A. & Lehane, B.M. (2007) Self-boring pressuremeter testing in Spearwood dune sands. Australian Geomechanics, v. 42:4, p. 57-71.

Fioravante, V.; Giretti, D.; Abate, G.; Aversa, S.; Boldini, D.; Capilleri, P.P.; Cavallaro, A.; Chamlagain, D.; Crespellani, T.; Dezi, F.; Facciorusso, J.; Ghinelli, A.; Grasso, S.; Lanzo, G.; Madiai, C.; Massimino, M.R.; Maugeri, M.; Pagliaroli, A.; Rainieri, C.; Tropeano, G.; Santucci De Magistris, F.; Sica, S.;Silvestri, F. & Vannucchi, G. (2013) Earthquake geotechnical engineering aspects of the 2012 Emilia-Romagna earthquake (Italy). Proc. 7th Int. Conf. on Case Histories in Geotechnical Engineering, Chicago, Paper No. EQ-5.

Gibbens, R.M. & Briaud, J.L. (1994a) Test and prediction results for five large spread footings on sand. Geotechnical Special Publication, ASCE, v. 41, p. 92-128.

Gibbens, R.M. & Briaud, J.L. (1994b) Data and prediction request for the spread footing prediction event (at the occasion of the ASCE Spec. Conf. Settlement '94). Geotechnical Special Publication, ASCE, v. 41, p. 11-85.

Gottardi, G. & Tonni, L. (2004) A comparative study of piezocone tests on the silty soils of the Venice lagoon (Treporti Test Site). Viana da Fonseca A. & Mayne P.W. (eds) Proc. 2nd International Conference on Site Characterization, Porto, v. 2, p. 1643-1649.

Hardin, B. O. & Drnevich, V. P. (1972) Shear modulus and damping in soils: design equations and curves. J. Soil Mech. and Found. Div., ASCE, v. 98:SM7, p. 667-692.

Hepton, P. (1988) Shear wave velocity measurements during penetration testing. Proc. Penetration Testing in the UK, ICE, p. 275-278.

Ishihara, K. (2001) Estimate of relative density from in-situ penetration tests. Rahardjo P.P. & Lunne T. (eds). Proc. Int. Conf. on *In Situ* Measurement of Soil Properties and Case Histories, Bali, p. 17-26.

Iwasaki, T.; Tatsuoka, F. & Takagi, Y. (1978) Shear moduli of sands under cyclic torsional shear loading. Soils and Foundations, v. 18:1, p. 39-56.

Jardine, R.J. (1992) Non-linear stiffness parameters from undrained pressuremeter tests. Can. Geotech. J., v. 29:3, p. 436-447.

Kokusho, T. (1980) Cyclic triaxial test of dynamic soil properties for wide strain range. Soils and Foundations, v. 20:2, p. 45-60.

Lehane, B.M. & Fahey, M. (2004) Using SCPT and DMT data for settlement prediction in sand. Viana da Fonseca A. & Mayne P.W. (eds) Proc. 2nd Int. Conf. on Site Characterization, Porto, v. 2, p. 1673-1679.

Lehane, B.M.; Mathew, G. & Stewart, D. (2007) A laboratory investigation of the upper horizons of the Perth/Guildford formation in Perth CBD. Australian Geomechanics, v. 42:3, p. 87-100.

Lehane, B.M. (2010) Shallow foundation performance in a calcareous sand. Proc 2nd Int. Symposium on Frontiers in Offshore Geotechnics, ISFOG-2, Perth, p. 427-432.

Marchetti, S. (1980) *In Situ* Tests by Flat Dilatometer. J. Geotech. Engrg. Div., ASCE, v. 106:GT3, p. 299-321.

Marchetti, S.; Monaco, P.; Totani, G. & Calabrese, M. (2001) The Flat Dilatometer Test (DMT) in Soil Investigations - A Report by the ISSMGE Committee TC16. Proc. 2nd Int. Conf. on the Flat Dilatometer, Washington D.C., p. 7-48.

Marchetti, S.; Monaco, P.; Calabrese, M. & Totani, G. (2004) DMT-predicted vs measured settlements under a full-scale instrumented embankment at Treporti (Venice, Italy). Viana da Fonseca A. & Mayne P.W. (eds) Proc. 2nd Int. Conf. on Site Characterization, Porto, v. 2, p. 1511-1518.

Marchetti, S.; Monaco, P.; Calabrese, M. & Totani, G. (2006) Comparison of moduli determined by DMT and backfigured from local strain measurements under a 40 m diameter circular test load in the Venice area. Failmezger R.A. & Anderson J.B. (eds) Proc. 2nd Int. Conf. on the Flat Dilatometer, Washington D.C., p. 220-230.

Marchetti, S.; Monaco, P.; Totani, G. & Marchetti, D. (2008) *In Situ* tests by seismic dilatometer (SDMT). Laier, J.E.; Crapps D.K. & Hussein M.H. (eds) From Research to Practice in Geotechnical Engineering. Geotechnical Special Publication, ASCE, v. 180, p. 292-311.

Martin, G.K. & Mayne, P.W. (1997) Seismic flat dilatometer tests in Connecticut Valley Varved clay. Geotech. Testing J., ASTM, v. 20:3, p. 357-361.

Martin, G.K. & Mayne, P.W. (1998) Seismic flat dilatometer in Piedmont residual soils. Robertson P.K. & Mayne P.W. (eds) Proc. 1st Int. Conf. on Site Characterization, Atlanta, v. 2, p. 837-843.

Mayne, P.W.; Schneider, J.A. & Martin, G.K. (1999) Small- and large-strain soil properties from seismic flat dilatometer tests. Jamiolkowski, M.; Lancellotta R. & Lo Presti D.C.F. (eds) Pre-failure Deformation Characteristics in Geomaterials. Balkema, Rotterdam, p. 419-427.

Mayne, P.W. (2001) Stress-strain-strength-flow parameters from enhanced in-situ tests. Rahardjo P.P. & Lunne T. (eds), Proc. Int. Conf. on *In Situ* Measurement of Soil Properties and Case Histories, Bali, p. 27-47.

Mayne, P.W. (2003) Class "A" footing response prediction from seismic cone tests. Proc. 3rd Int. Symp. Deform. Charact. Geomaterials, Lyon, v. 1, p. 883-888.

McGillivray, A. & Mayne, P.W. (2004) Seismic piezocone and seismic flat dilatometer tests at Treporti. Viana da Fonseca A. & Mayne P.W. (eds) Proc. 2nd Int. Conf. on Site Characterization, Porto, v. 2, p. 1695-1700.

Monaco, P.; Totani, G. & Calabrese, M. (2006) DMT-predicted vs observed settlements: a review of the available experience. Failmezger R.A. & Anderson J.B. (eds) Proc. 2nd Int. Conf. on the Flat Dilatometer, Washington D.C., p. 244-252.

Monaco, P.; Totani, G.; Barla, G.; Cavallaro, A.; Costanzo, A.; D'Onofrio, A.; Evangelista, L.; Foti, S.; Grasso, S.;

Lanzo, G.; Madiai, C.; Maraschini, M.; Marchetti, S.; Maugeri, M.; Pagliaroli, A.; Pallara, O.; Penna, A.; Saccenti, A.; Santucci de Magistris, F.; Scasserra, G.; Silvestri, F.; Simonelli, A.L.; Simoni, G.; Tommasi, P.; Vannucchi, G. & Verrucci, L. (2012) Geotechnical aspects of the L'Aquila earthquake. Sakr M.A. & Ansal A. (eds) Special Topics in Advances in Earthquake Geotechnical Engineering, Chapter 1. Springer Science+Business Media B.V.

Monaco, P.; Totani, G.; Amoroso, S.; Totani, F. & Marchetti, D. (2013) Site characterization by seismic dilatometer (SDMT) in the city of L'Aquila. Rivista Italiana di Geotecnica, v. XLVII:3, p. 8-22.

Monaco P.; Amoroso S.; Marchetti S.; Marchetti D.; Totani G.; Cola S. & Simonini P. (2014) Overconsolidation and Stiffness of Venice Lagoon Sands and Silts from SDMT and CPTU. J. Geotech. Geoenviron. Eng., ASCE, v. 140:1, p. 215-227.

Regione Emilia Romagna - Liquefaction Working Group (2012) Primo rapporto sugli effetti della liquefazione osservati a S. Carlo, frazione di S. Agostino (Provincia di Ferrara). 25 June 2012 (in Italian), http://ambiente.regione.emilia-romagna.it/geologia/temi/sismica/liquefazione-gruppo-di-lavoro/rapporto_sancarlo.pdf/at_download/file/rapporto_sancarlo.pdf.

Robertson, P.K. & Ferrera, R.S. (1993) Seismic and pressuremeter testing to determine soil modulus. Predictive soil mechanics, Wroth Memorial Symposium, p. 562-580.

Romeo, R. W.; Amoroso, S.; Facciorusso, J.; Lenti, L.; Madiai, C.; Martino, S.; Monaco, P.; Rinaldis, D. & Totani, F. (2015) Soil liquefaction during the Emilia, 2012 seismic sequence: investigation and analysis. Engineering Geology for Society and Territory - Urban Geology, Sustainable Planning and Landscape Exploitation, Springer International Publishing, v. 5:XVIII, p. 1107-1110.

Santucci de Magistris, F.; d'Onofrio, A.; Evangelista, L.; Foti, S.; Maraschini, M.; Monaco, P.; Amoroso, S.; Totani, G.; Lanzo G.; Pagliaroli, A.; Madiai, C.; Simoni, G. & Silvestri, F. (2013) Geotechnical characterization of the Aterno valley for site response analyses. Rivista Italiana di Geotecnica, v. XLVII:3, p. 23-43.

Schneider, J.A.; Fahey, M. & Lehane, B.M. (2008) Characterization of an unsaturated sand deposit by *in situ* testing. Proc. 3rd Int. Conf. on Site Characterization, p. 633-638.

Schneider, J.A. & Lehane, B.M. (2010) Evaluation of cone penetration test data from a calcareous sand dune. Proc. 2nd Int. Symp. on Penetration Testing, Huntington Beach, CA.

Seed, H.B.; Wong, R.T.; Idriss, I.M. & Tokimatsu, K. (1986) Moduli and damping factors for dynamic analyses of cohesionless soils. Journal of the Soil Mechanics and Foundations Division, ASCE, v. 112:SM11, p. 1016-1032.

Simonini, P. (2004) Characterization of the Venice lagoon silts from in-situ tests and the performance of a test embankment. Viana da Fonseca A. & Mayne P.W. (eds) Proc. 2nd Int. Conf. on Site Characterization, Porto, v. 1, p. 187-207.

Simonini, P.; Ricceri, G. & Cola, S. (2006) Geotechnical characterization and properties of the Venice lagoon heterogeneous silts. Proc. 2nd Int Workshop on Characterization and Engineering Properties of Natural Soils, Singapore, v. 4, p. 2289-2328.

Sun, J.I.; Golesorkhi, R. & Seed H.B. (1988) Dynamic Moduli and Damping Ratio for Cohesive Soils. Report, UCB/EERC-88/15, University of California at Berkley, 48 p.

Totani, G.; Totani, F.; Monaco, P.; Tallini, M.; Del Monaco, F. & Zia, G. (2012) Site investigations and geotechnical problems in the Southern part of the historic centre of L'Aquila. Maugeri M. & Soccodato C. (eds) Proc. 2nd Int. Conf. on Performance-Based Design in Earthquake Geotechnical Engineering, Taormina, Italy, Paper No. 2.13, p. 315-328 (CD-ROM).

Vucetic, M. & Dobry, R. (1991) Effect of soil plasticityon cyclic response. Journal of Geotechnical Engineering, ASCE, v. 120:7, p. 585-594.

Working Group S2-UR4 (2013) Analysis of the liquefaction phenomena in the area of San Carlo by seismic dilatometer (SDMT). Project S2-2012 INGV-DPC, Deliverable D8.1 - Annex 3, Rev. 1.1, Sept. 2013 https://docs.google.com/file/d/0B60wsWaPpDL4RVMzb01ETU8zT2s/edit?usp=sharing.